World Journal of Advanced Engineering Technology and Sciences
eISSN: 2582-8266
Cross Ref DOI: 10.30574/wjaets
Journal homepage: https://wjaets.com/

(RESEARCH ARTICLE)

Check for updates

HYDROGEN RESERVE STORAGE SELECTION UNDER RESTORATION CONSTRAINTS AND COST UNCERTAINTY

Rawail Saeed [1,*] and Syed Zeeshan [2]

[1] Southern New Hampshire University, Manchester, New Hampshire, USA.
[2] Department of Chemical Engineering, NED University of Engineering and Technology, Karachi, Sindh, Pakistan.
* Corresponding Author

World Journal of Advanced Engineering Technology and Sciences, 2026, 21(02), 202–213

Publication history: Received on 03 October 2026; revised on 10 November 2026; accepted on 12 November 2026

Article DOI: https://doi.org/10.30574/wjaets.2026.21.2.0501

Copyright © 2026 Author(s) retain the copyright of this article. This article is published under the terms of the Creative Commons Attribution License 4.0

ABSTRACT

Choosing hydrogen reserve storage requires knowing whether the reserve can be restored and whether the available equipment costs apply to the intended service. We develop a reproducible screening framework for a stationary 1,000 kg H_2 day^{-1} service at 20 bar and 15 °C, with 1–90 days of reserve and 1–30 days for restoration. A common discounted-cash-flow model accounts for mass-conserving inventory trajectories and hydrogen working capital. Compressed gas at 350 bar and liquid hydrogen form the main decision set; hydrides are treated as conditional performance cases. Across 10,000 exploratory draws, the reference gas–liquid crossover has a median of 55.26 days. Substituting stationary cost estimates shifts this median to 9.48–14.58 days, a larger change than the numerical sampling variation. No probabilities are assigned to source families. Worst-case regret across their declared capital boxes favors gas at 1–7 days and liquid at 30–90 days, provided operation is feasible. A published production-capacity benchmark shows why this matters. With assumed demand of 1,000 kg/day and supply capped at 1,200 kg/day, a 90-day gas reserve takes at least 450 days to restore. Checks on power, availability, and low-load operation further limit what cost rankings alone can establish. The framework identifies choices that depend on the stated conditions and the evidence needed to assess them. It does not establish a universal switching duration. Matched installed costs and operating records are still needed for project deployment.

Keywords: Hydrogen Reserve; Restoration Window; Technoeconomic Analysis; Capital Uncertainty; Global Sensitivity; Minimax Regret

1 INTRODUCTION

Reserve storage maintains a specified hydrogen service during a supply interruption. The system must provide enough deliverable hydrogen throughout the interruption and then restore the reserve within the allowed recovery window. Longer reserve autonomy requires more inventory, while faster restoration requires more conditioning capacity. Comparisons based only on storage density or annual throughput can overlook this relationship [1–3].

Recent studies examine hydride economics, integrated stationary-plant optimization, and reproducible comparisons of compressed, liquid, and geological storage [4,5,14]. Here, we combine an explicit inventory trajectory with separate assessments of bounded engineering uncertainty, installed-cost uncertainty, and the consequences of technology

selection. We check source, conditioning, and utility capacity before interpreting cost rankings. The analysis identifies conditional decision boundaries and evidence needs for above-ground storage. It does not establish a universal economic switching duration or introduce a new storage material.

2 SERVICE DEFINITION AND INVENTORY CONSERVATION

The facility delivers qd = 1,000 kg day^{-1} at 20 bar and 15 °C, with the same gas state at the inlet. In one annual reserve exercise, external supply stops for D days. The reserve is then restored over W days and held full for H = 365 − D − W days. All analyzed cases satisfy H ≥ 0, with annual delivery of 365,000 kg. The facility boundary excludes upstream hydrogen production and downstream use but includes loss replacement and financing of the initial retained hydrogen inventory. Figure 1 shows the common comparison boundary.

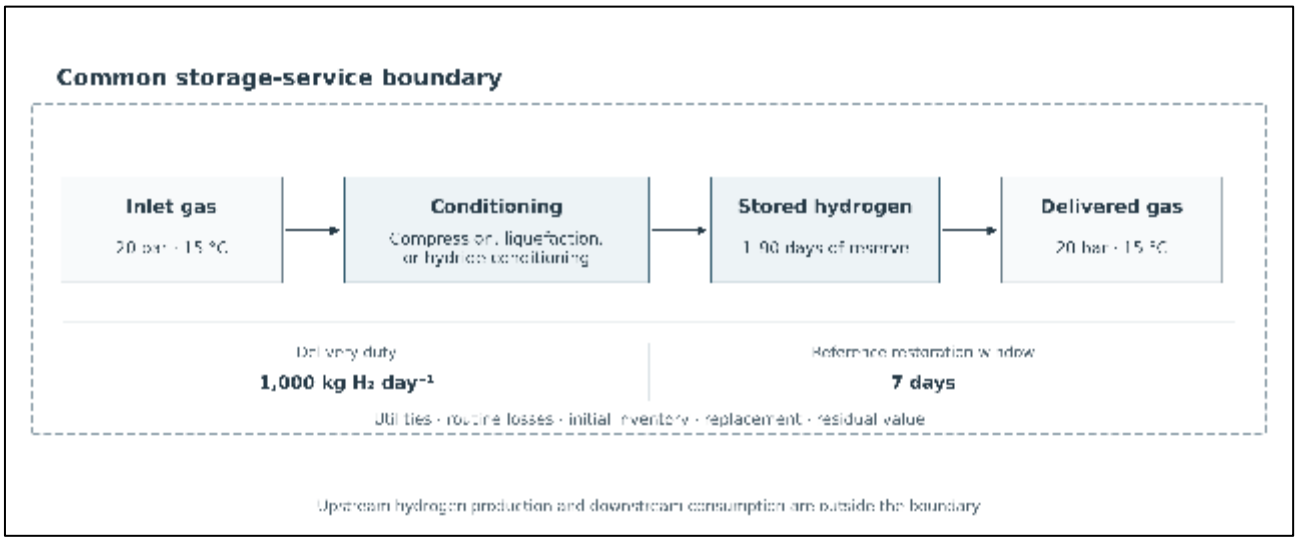


Figure 1: Common facility boundary. Reserve inventory supports continuous delivery. Conditioning capacity covers both reserve restoration and ongoing delivery; utility use is integrated over the annual schedule.

For gas without modeled standing leakage, usable reserve mass is Mu = qdD and restoration feed is qc = qd + Mu/W. Cryogenic restoration must also replace hydrogen lost during the supply interruption. The baseline uses a constant loss rate φM0, where M0 is the full nominal liquid inventory and h = 0.05 is the heel fraction. The mass remaining at the end of discharge is hM0:

$$M0 - qdD - \varphi M0D = hM0; \quad M0 = qdD / (1 - h - \varphi D).$$

$$qc = qd + (1 - h)M0/W + \varphi M0; \quad M_{ann,loss} = 365\varphi M0.$$

The restoration term covers the full inventory swing (1 − h)M0. Using qdD instead would omit losses during the reserve period. At D90/W7 and φ = 0.0005 day^{-1}, the corrected design requires 99,447.51 kg of nominal liquid inventory and 14.546 t day^{-1} of total feed. The annual feed balance, qcW + (qd + φM0)H = 365qd + Mann,loss, links the design flow to annual energy use.

The functional unit is one kilogram of continuously delivered service. Allocating the same annualized cost only to delivery during the reserve exercise would multiply LCOHS by 365/D. This changes neither physical operation nor the ranking at a fixed D, but it affects comparisons between service definitions. Reported costs must therefore state both the denominator and the reserve autonomy.

3 ENGINEERING AND HYDRIDE FEASIBILITY

The gas working inventory is V[ρ(350 bar,T) − ρ(20 bar,T)], using normal-hydrogen densities of 23.99475 and 1.66284 kg m^{-3} at 288.15 K from the retained CoolProp 8.0.0 calculation [7,8]. D90 requires 4,030.11 m^3 of internal vessel volume. Compression uses three stages and an electrical-work relation K/η fitted to the retained real-gas grid over η = 0.70–0.80. These capacities are screening estimates. Installation layout, redundancy, and safety clearances require separate design.

The liquid case uses a 0.90 fill fraction, a para-hydrogen density of 70.8281 kg m^{-3}, liquefaction energy of 10–13 kWh kg^{-1}, and 0.026 kWh kg^{-1} for delivery pumping and vaporization auxiliaries [6–8]. Applying the same fractional loss to different tank sizes implies different heat loads per unit area. This assumption defines an engineering envelope, not a validated tank heat-transfer model [9].

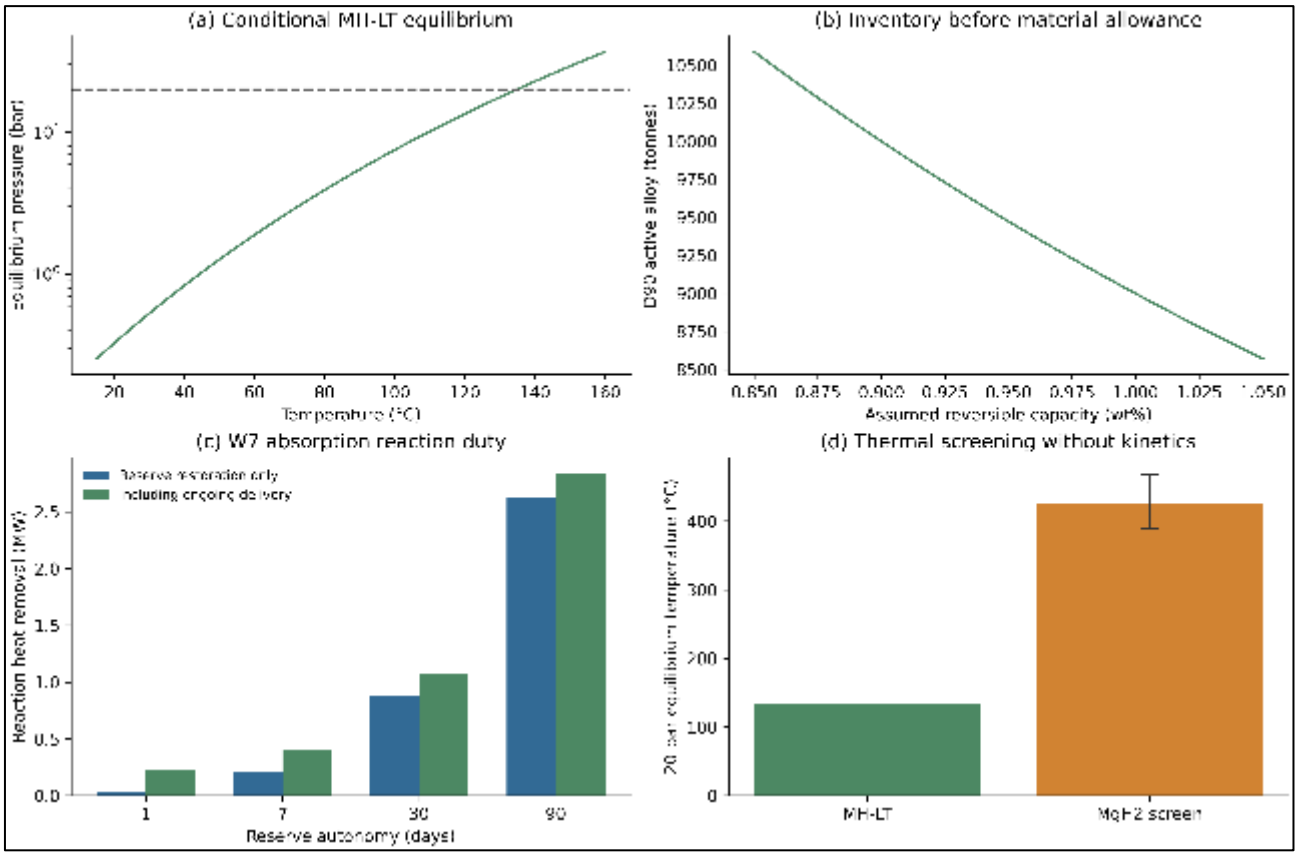


Figure 2: Hydride screening from retained engineering inputs. Equilibrium pressure does not establish discharge kinetics or working capacity. Alloy inventories exclude the separate upfront material allowance. Reaction-duty bars use 4.90756 kWhth kg^{-1} and explicit hydrogen flow; sensible heating and auxiliary loads are excluded. MgH_2 remains an engineering-only case.

MH-LT represents $La_{0.41}Ce_{0.59}Ni_{3.71}Co_{0.52}Mn_{0.36}Al_{0.29}$ [12]. Its assumed working capacity of 0.0093947 kg H_2 kg^{-1} at 20 bar relies on extrapolation. Neither lower-pressure measurements nor pure-$LaNi_5$ uptake validates this operating window [12,13]. At D90/W7, reaction-only absorption duty is 2.629 MW for reserve restoration and 2.834 MW when ongoing delivery is included. Delivery reaction duty is 0.2045 MW. The amount of alloy purchased is Mu(1 + fdeg)/crev, and the bed included in the cost model holds all purchased material. Positive-mass and thermodynamic checks alone do not show that a reactor can operate as required, so hydride economic rankings remain conditional.

4 ECONOMIC ACCOUNTING AND COST EVIDENCE

All costs use a constant 2023-dollar modeling basis. The pre-tax analysis assumes a 20-year horizon and a 7% real discount rate. Let C0 denote installed hardware, I0 the initial hydrogen inventory purchase, Ay annual variable expenses, Fy fixed maintenance expenses, Ry replacement expenditure, and SN the terminal recovery of hardware and hydrogen. The storage-service cost is:

$$LCOHS = [C0 + I0 + \Sigma y{=}1\ldots20\ (Ay + Fy + Ry)/(1.07)^{y} - SN/(1.07)^{20}] \,/\, [365{,}000\ \Sigma y{=}1\ldots20\ (1.07)^{-y}].$$

Hydrogen working capital is charged at time zero, and the stated recovery is credited at year 20. Hydrogen inventory is excluded from the hardware O&M base. Gas inventory is fully recoverable; liquid recovery excludes the heel, and the conditional hydride case recovers its usable hydrogen. Hardware O&M is 3% of original installed capital, plus an additional 3% of replacement capital from year 15 onward. A separate scenario removes this additional O&M term because replacement need not increase the maintained asset base.

Gas hardware includes the compressor, vessels, 15% balance of plant, and 38% project indirects. Liquid hardware includes the liquefier, tank, 10% balance of plant, and the same indirects. Hydride hardware includes the alloy, reactor, thermal auxiliaries, balance of plant equal to 20% of reactor cost, and indirects. Compression equipment is replaced in year 15. The inherited liquid model replaces balance of plant, while the hydride case replaces thermal auxiliaries, balance of plant, and half the reactor basis. Salvage follows the retained component lives of 15, 30, and 40 years. These are accounting scenarios, not forecasts of actual maintenance or asset resale.

Table 1: Cost-anchor scope. CEPCI indices follow the publisher's annual table [11]. Trailer estimates are transferred to stationary service. The DOE liquefier equation already includes installation; the inherited extra factor 1.12 is tested separately in S15. The common BOP, indirects, and anchor vintages remain scope assumptions. Section 10 evaluates alternative stationary sources.

Component	Screening cost basis	Evidence qualification
Gas storage	783 USD/kg gross capacity; replicated linearly	Trailer comparison; stationary scope and assigned 2015 vintage unverified [15]
Liquid tank	167 USD/kg at an assumed 4.3-t reference; exponent 0.5–1.0	The cited numerical anchor describes a liquid trailer [15]
Liquefier	$5.6 \times 10^6 \times Q^{0.8}$; inherited adjustments and 2016 escalation	Federal cost basis; extrapolated below 6 t/day [10]
Hydride	20 USD/kg alloy; reactor 12,000 and auxiliaries 2,500 USD/m^3	Alloy price is a literature assumption [4]; reactor rates are engineering assumptions
Compressor	$63{,}000 \times P^{0.46}$; inherited installation and vintage adjustments	Screening relation; exact coefficient vintage and package scope require confirmation

ORNL's vendor-informed steel/concrete composite vessel estimates provide a separate stationary cross-check [22]. Taking 2012 as the report-year cost basis and multiplying by 797.9/584.6 gives approximately 934–973 USD/kg at 430 bar and 1,254–1,306 USD/kg at 860 bar in 2023 dollars. The endpoints represent projected friction-stir welding and conventional welding, not uncertainty percentiles. Because SCCV construction, pressure, and cost scope differ, the comparison can only corroborate the cost scale. It neither validates nor replaces a model coefficient. S21 explains the comparison and its price-year caveat.

Electricity is fixed at 0.0804 USD kWh^{-1}, the EIA 2023 industrial average [17]. The natural-gas value of 4.467 USD per thousand cubic feet is retained as a scenario input and is not presented as the official annual volume-weighted price. Heat calculations use 1.037 MMBtu per thousand cubic feet, 293.07 kWh per MMBtu, and a heater efficiency of 0.85. Cooling costs 0.003 USD $kWhth^{-1}$, and hydrogen is valued at 2 USD kg^{-1}. These tariffs are fixed in all reported uncertainty experiments. Separate accounting scenarios include initial-fill conditioning energy and consistently exclude project indirects from residual-value terms. Within each cost family, these scenarios leave the median gas–liquid ordering unchanged at the four analyzed durations. Supporting Information S19 gives the full results.

5 UNCERTAINTY AND DECISION ANALYSIS

The baseline uses six independent exploratory uniform inputs and fixed capital coefficients. The 10,000 parameter sets come from the first six columns of the retained eight-column randomized Latin-hypercube design, generated with seed 20261019. Each column contains exactly one point in each of 10,000 strata. The other two columns describe high-temperature-hydride thermal quantities and do not affect the three economic cases. We therefore report six active economic variables, while retaining the full design for traceability.

A separate four-column Latin-hypercube design, generated with seed 20261021, varies the capital inputs alongside the six baseline variables. Each hardware change carries through to the associated balance of plant, indirects, replacement, and salvage. The main recommendations compare CG350 with LH_2. Positive hydride costs alone do not establish performance eligibility. For technology i and scenario θ, regret is $R_i(\theta) = C_i(\theta) - \min_j C_j(\theta)$. Mean regret averages over the selected exploratory laws. Worst-case regret takes the maximum over a capital-cost box with engineering variables fixed. With engineering fixed, cost is affine in the four capital coordinates, so pairwise differences reach their extrema among the 16 vertices. Minimax regret requires no probability distribution within this box.

Table 2: Active inputs. Uniform sampling assigns a numerical measure to each bounded range without establishing an empirical probability law. Hydride working capacity is fixed and conditional. MH-LT is excluded from the main recommendation set, and its costs describe a performance scenario. Using the same parameter set across durations keeps the uncertain design properties consistent. Technology-specific columns are independent. Matching draw indices allows a joint comparison under that product-law assumption; it does not imply a measured cross-technology correlation.

Input	Range	Treatment and basis
Compressor efficiency η	0.70–0.80	Engineering machine-class envelope
Liquefaction SEC	10–13 kWh/kg	Between-plant screening range [6,10]
Liquid loss fraction φ	0.0001–0.0005 day^{-1}	Assumed insulation-class screening envelope
Liquid-tank cost exponent b	0.50–1.00	Engineering range around a 2/3 geometric basis
Hydride bed packing density	4.5–5.5 t/m^3	Engineering assumption
Upfront hydride allowance fdeg	0.05–0.30	Additional installed material; exploratory assumption
Gas vessel capital multiplier	0.70–1.30	Capital experiment only; uncalibrated support
Liquefier capital multiplier	0.50–2.00	Capital experiment only; uncalibrated support
Hydride reactor and aux multiplier	0.50–2.00	Capital experiment only; uncalibrated support
Hydride alloy price	10–30 USD/kg	Capital experiment only; assumption band [4]

We evaluate the global sensitivity of the D90 paired liquid-minus-gas difference using Jansen variance estimators [16], with 8,192 points in each of two scrambled Sobol input blocks. Ten inputs are assessed across four independent scrambles. Hydride-only variables have zero effect on this pairwise response by construction. The replicate ranges measure numerical variation, not uncertainty in the selected input supports.

6 BASELINE COSTS AND DURATION CROSSOVER

CG350 has the lower median at 1, 7, and 30 days. At 90 days, the median paired advantage for LH_2 is 6.45 USD kg^{-1}. The liquid-minus-gas difference has a mean of −5.90 and a P5–P95 interval of −9.32 to −0.98 USD kg^{-1}. LH_2 is cheaper in 9,895 of 10,000 paired draws; the remaining 105 favor CG350. This 98.95% frequency describes the declared baseline sampling law, not a market probability.

Bisection for each draw over 1–120 days gives a crossover median of 55.26 days and a P5–P95 interval of 46.64–81.96 days. A separate 321-point logarithmic scan finds one sign change per draw. Its interpolated roots differ from the bisection roots by less than 0.001 day, and the maximum absolute cost residual at the bisection root is below 1.1×10^{-11} USD kg^{-1}. These checks establish numerical resolution within the continuous model. A commercial design may have discrete vessels or liquefier trains, redundancy requirements, and operating limits that prevent a smooth or unique crossover.

Table 3: Median [P5–P95] baseline storage-service cost in constant 2023 USD kg^{-1}. Intervals reflect only the six specified inputs with capital fixed. Positive hydride costs do not establish feasibility at the delivery condition.

Reserve days	CG350	LH_2	MH-LT conditional
1	1.27 [1.24–1.29]	6.99 [6.86–7.12]	1.50 [1.37–1.64]
7	5.11 [5.09–5.14]	10.92 [10.77–11.08]	9.88 [8.94–10.81]
30	19.65 [19.61–19.69]	23.46 [22.60–24.79]	42.00 [37.96–46.00]
90	57.16 [57.11–57.22]	50.71 [47.83–56.19]	125.79 [113.68–137.80]

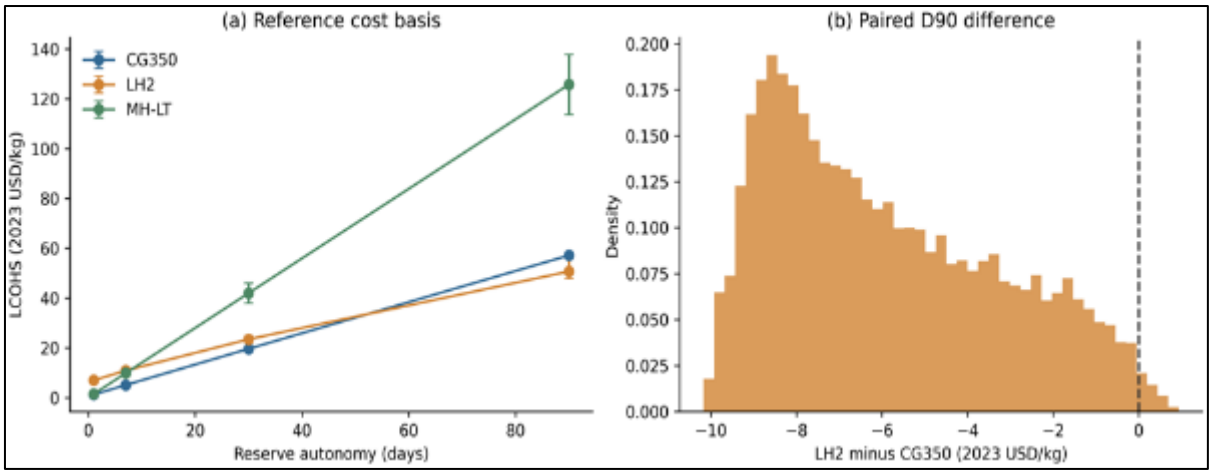


Figure 3: Reference-cost results and the D90 paired cost difference. The histogram includes the small positive tail. Negative differences favor liquid hydrogen. Lines connecting the four reserve durations guide the eye. Crossover locations come from the continuous evaluator, not the plotted segments.

Four independent 10,000-point Latin-hypercube runs give crossover medians of 55.19–55.26 days, compared with 55.26 days in the retained design. Their crossover P95 values span 82.04–82.21 days. This numerical spread is much smaller than the modeled uncertainty range, but it does not reduce uncertainty in cost-anchor scope or hydride performance.

7 RESTORATION TIME AND COST THRESHOLDS

The restoration window sets peak conditioning duty separately from stored inventory. At D90, shortening W from 30 to 1 day increases median LH_2 cost from 22.83 to 206.25 USD kg^{-1}. CG350 cost changes from 56.44 to 59.43, and cost in the conditional hydride case changes from 125.77 to 126.01. The large liquid response reflects the costed liquefier capacity. The small hydride response also exposes a model limitation. Reactor cost scales with bed volume, with no independently calibrated allowance for heat-transfer area or a rate-dependent reactor premium.

With engineering inputs fixed, gas and liquid costs can be written as Cg = ag + bgvg and Cl = al + blvl, where vg and vl are the vessel and liquefier multipliers, respectively. Equality gives vl* = (ag + bgvg − al)/bl. At D90 with vg = 1, vl* is 1.153. Increasing liquefier capital by approximately 15.3% relative to the inherited baseline therefore removes the deterministic liquid advantage. This threshold includes the linked capital, O&M, replacement, and salvage effects. It shows where better cost evidence could change the choice; it is not a quote tolerance for an unspecified package.

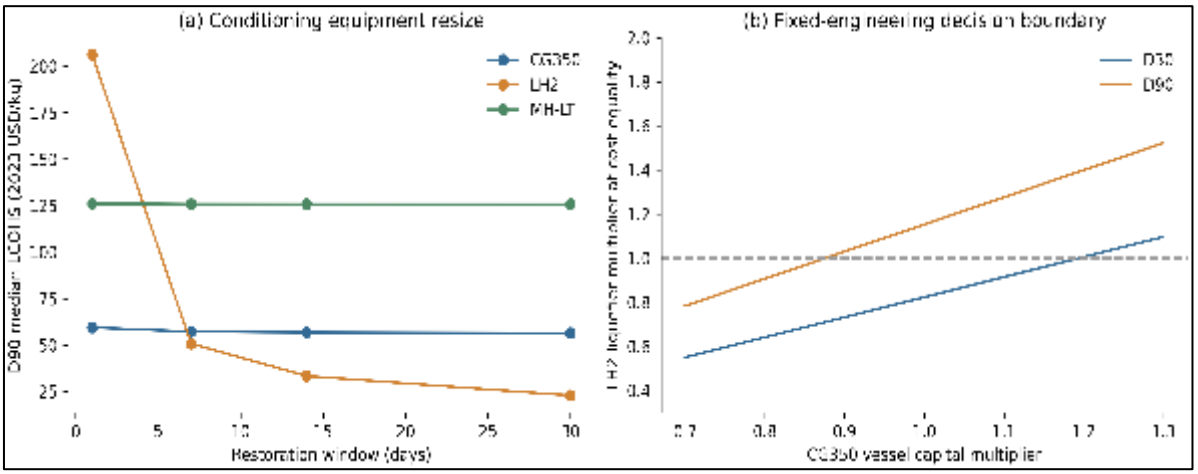


Figure 4: Recharge-window response and fixed-engineering capital thresholds. In panel b, LH_2 is cheaper below the relevant equality line and CG350 above it. Engineering and cost inputs not plotted are fixed. The lines are analytical repricing boundaries for the stated equipment scope.

Table 4: Distribution-free sensitivity to cost-box expansion at fixed engineering. The box is Cpin + γ(Cbox − Cpin), with γ = 0 at the baseline and γ = 1 at the full ranges in Table 2. The reported γ is the first point at which any gas–liquid cost reversal becomes possible. At D90, γ = 0.112 corresponds to about −3.35% in vessel capital combined with +11.18% in liquefier capital along the adverse vertex. This is a joint variation, not an independent 11.2% uncertainty interval.

Reserve days	Pinned gas–liquid preference	First reversal fraction γ
1	CG350	No reversal within box
7	CG350	0.982
30	CG350	0.229
90	LH2	0.112

8 CAPITAL UNCERTAINTY AND THE CONSEQUENCE OF A WRONG CHOICE

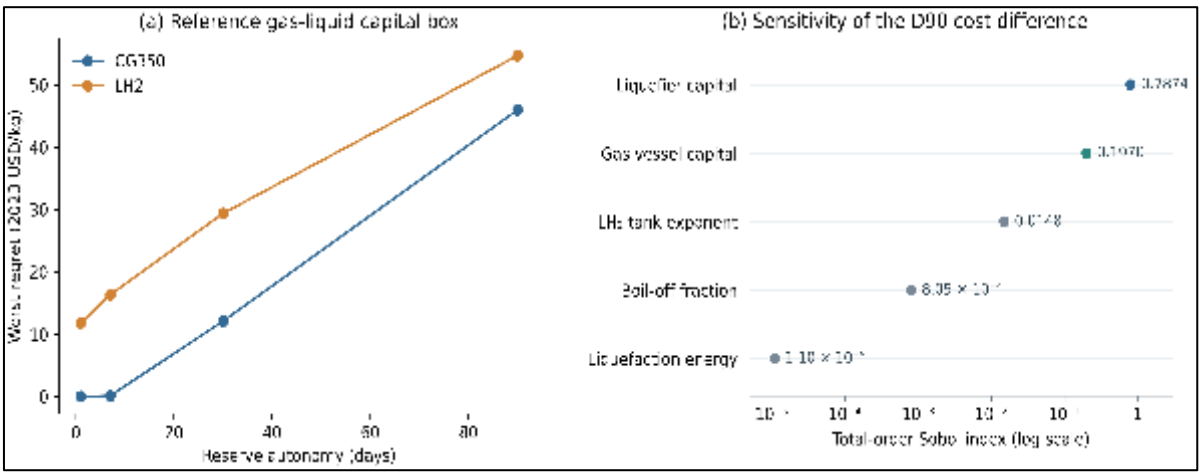


Figure 5: Effects of capital uncertainty on technology choice. Panel a gives exact gas–liquid worst-case regret within the reference capital box, with engineering inputs fixed. Hydride-only capital coordinates do not affect this comparison. Panel b gives mean total-order Sobol indices for the D90 liquid-minus-gas difference under the exploratory product laws. The chosen input ranges determine these indices.

When MH-LT is excluded from the primary decision set, expanded capital uncertainty at D90 gives minimum-cost frequencies of 58.06% for CG350 and 41.94% for LH_2 under the reference cost basis. Both the support and the numerical weighting of the cost assumptions differ from those in the baseline. Uniform liquefier multipliers over 0.5 to 2.0, for example, have a mean of 1.25. The experiment raises the central capital level as well as widening uncertainty, so variance alone cannot explain the change in ranking.

Table 5: Regret in 2023 USD kg^{-1}. The first two columns integrate capital and engineering draws. The last column comes from a separate experiment using exact capital-box vertices with engineering fixed. It is not a percentile of the sampled distribution.

D90 technology	Mean regret	P95 regret	Cost-box worst regret
CG350	6.66	29.99	45.97
LH2	11.83	39.76	54.68

Within the reference cost family, CG350 minimizes gas–liquid worst-case regret at all four durations, even though LH_2 has the lower baseline D90 median. At D90, worst-case regrets are 45.97 and 54.68 USD kg^{-1} for gas and liquid, respectively. This preference reflects a decision maker seeking protection across the full selected box. It does not establish that gas is commercially superior. Section 10 tests whether the preference holds under alternative stationary cost evidence. Hydride cases remain outside the recommendation set until matched performance evidence is available.

Liquefier capital has a total-order index of 0.7874 and vessel capital has an index of 0.1970, giving a sum of approximately 0.9844. The liquid-tank exponent contributes 0.0148. Boil-off and energy inputs contribute much less

over their selected supports. In this experiment, matched capital evidence is more likely to change the technology choice than tighter numerical sampling or more precise estimates of electricity consumption. This priority depends on the chosen cost ranges, fixed tariffs, and annual service definition.

9 OPERATING CONSTRAINTS BEFORE ECONOMIC SELECTION

Before interpreting storage costs, we check whether the reserve can be restored. Let F denote firm source supply, Q the available conditioning rate, P the conditioning power limit, e the specific energy, and a the conditioning availability. A necessary average-throughput bound is K = min(F, aQ, 24aP/e), in kg/day. For gas, Wmin = qdD/(K − qd). For the constant-nominal liquid model, Wmin = (1 − h)M0/(K − qd − φM0). Restoration is impossible when the denominator is nonpositive. If D + Wmin > 365, the prescribed annual cycle is also impossible. These necessary bounds do not account for auxiliary loads, start-up, or clustered downtime, which require further design evidence.

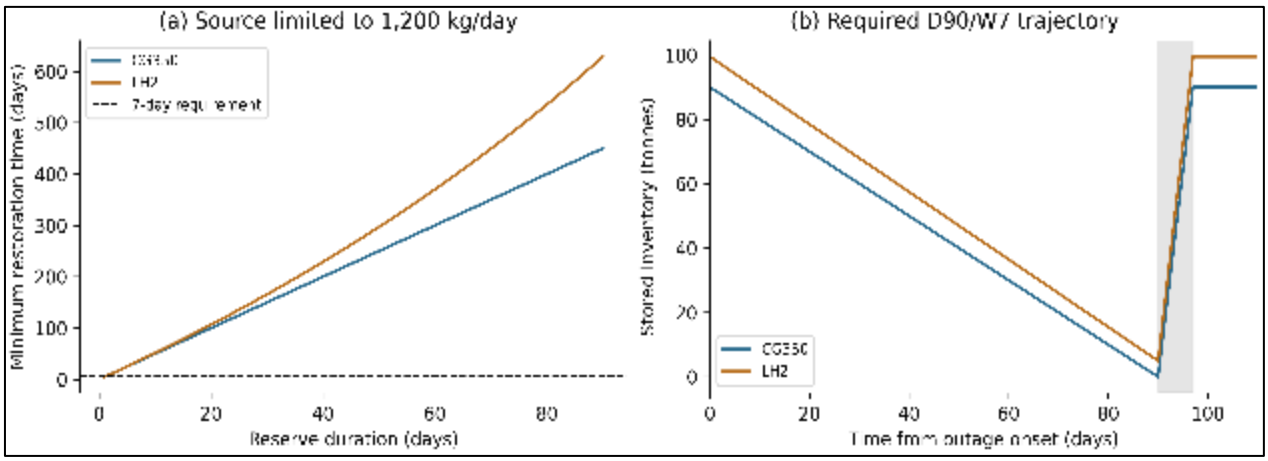


Figure 6: Capacity and inventory checks. Panel a combines a published production-capacity scale with assumed demand; it does not describe actual site operations. Panel b shows the mass-conserving D90/W7 trajectory, which requires sufficient supply and conditioning. Shading marks restoration. Gas inventory is usable reserve, while liquid inventory includes the heel.

A DOE account of the operating Long Beach Tri-gen facility reports access to hydrogen production capacity of up to 1,200 kg/day [21]. We combine this published scale with the study's assumed demand of 1,000 kg/day. At D90, restoration takes at least 450 days for gas and 629 days for liquid at the fixed loss rate. Neither case can meet the annual D90/W7 service. This is a counterfactual capacity benchmark. It does not validate the facility's actual demand, pressure or reserve policy.

A separate illustrative site case assumes source supply of 20 t/day and conditioning capacity of 15 t/day. A 1 MW compressor limit allows the fixed D90/W7 gas throughput. A 5 MW liquefier limit, however, requires at least 10.07 days at 11.5 kWh/kg, before additional auxiliary loads are included. At 90% conditioning availability, the necessary windows increase to 7.20 days for gas and 11.33 days for liquid. A 14-day requirement passes these average capacity checks but does not establish chronological operability.

Low-load operation remains an unresolved constraint. At D90/W7, holding a full tank requires only 7.2% of peak liquefier throughput. This operating fraction therefore falls below the illustrative minimum-stable fractions of 10%, 25%, and 50%. Cycling would need a separately designed buffer or a revised reserve policy. A 20% SEC penalty during normal holding increases the paired liquid cost by a median of 0.140 USD/kg but does not resolve the operability failure. The supplement gives the detailed loss-law, discrete-equipment, source-scope, and availability experiments.

10 STATIONARY COST EVIDENCE AND MODEL APPLICABILITY

NREL reports an uninstalled 2022 rate of 1,750 USD/kg for Type I storage at 200–350 bar, with an installation factor of 1.3 [18]. We normalize this component rate to 2023 and substitute it into the common model, retaining its BOP, indirects, and financing. The interpretation as gross capacity and the replication across a large array remain assumptions. This substitution tests a source-based structural case; it is not a supplier quotation.

A second case also substitutes the correlation for installed stationary liquid tanks C = (3,100V + 5,646,600) × CEPCI2023/CEPCI2016, where V is water volume in m^3 [19]. Its lower applicability limit remains unresolved. The later

bottom-up study examines tanks of 5,000–100,000 m^3 [20], larger than the present D90 tank. This alternative correlation tests sensitivity to cost scope without providing independent empirical validation.

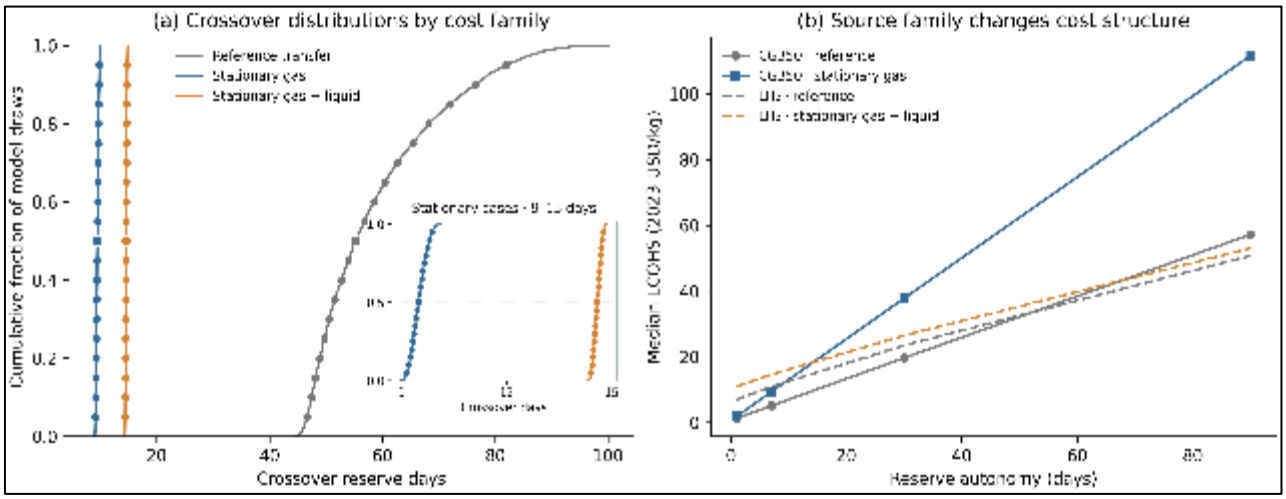


Figure 7: Effects of source family with the same engineering draws and service boundary. Panel (a) shows cumulative distributions of 10,000 crossover draws per family, with 19 percentile markers from P5 to P95 and larger median markers. Fractions reflect the exploratory sampling law. Distributions within each family do not include uncertainty about which source applies. Shorter-duration crossings extrapolate the liquefier relation below 6 t/day. A narrower interval does not demonstrate greater accuracy.

Table 6: Source-scope scenarios in 2023 USD/kg. Within-family crossover medians span 9.48–55.26 days; no probability is assigned to the choice of a cost family. The gas-only substitution isolates one anchor while retaining the reference liquid cost model.

Cost family	D90 gas median	D90 liquid median	Crossover median days
Reference transfer	57.16	50.71	55.26
Stationary gas	111.54	50.71	9.48
Stationary gas and liquid	111.54	53.02	14.58

Across the union of all three source families and their capital-box vertices, gas minimizes worst-case regret at D1 and D7, while liquid does so at D30 and D90. At D90, worst-case regrets are 116.67 USD/kg for gas and 54.68 for liquid. This reverses the preference found within the reference box alone. The selected source set still cannot cover every commercial design or missing cost item

11 DISCUSSION AND RELATION TO EXISTING WORK

The results separate a conditional cost crossover from a choice that remains defensible when cost structure is poorly known. Longer reserve autonomy increases retained-inventory cost, while shorter restoration time increases conditioning-capacity cost. Under the inherited gas replication law, vessel capital is approximately proportional to inventory. For liquid storage, liquefier capital increases with restoration flow and tank capital grows sublinearly. These relationships produce the modeled crossover. Its location changes with the cost scope, restoration window, or sizing law.

The baseline CG350 interval is narrow because the dominant vessel cost is fixed while compressor efficiency is sampled. It does not indicate precise knowledge of total installed cost. Broader capital ranges allow more possible outcomes but do not empirically calibrate their frequencies. The bounds need justification regardless of whether uncertainty is described by a probability law or a probability-free cost box. Reporting the boundary coefficients and first-reversal fraction lets readers examine these assumptions.

Wang et al. assess hydride system economics [4], Ademollo et al. compare integrated stationary plants [5], and Griñán and Gómez-Acebo provide a reproducible comparison of compressed, liquid, and cavern storage [14]. These studies show why integration and utilization matter. Our analysis builds on this work by linking prescribed reserve service and restoration duty to repricing thresholds and regret under a declared cost box.

Evidence from operating facilities also needs consistent comparison boundaries. Chao et al. use DTE Hydrogen Technology Park operating data and costs to model hypothetical 100–1,200 kg/day Park-like facilities, obtaining LCOH of 12.33–21.32 USD/kg in 2005 dollars [23]. These estimates include electrolysis, storage, dispensing, and associated costs. They offer historical system context but neither measure storage-only LCOHS nor validate our 2023-dollar results. They therefore cannot calibrate a storage coefficient. Geological options are outside the present above-ground design space; this does not imply that they are inferior where suitable sites exist [3,14].

The reference gas coefficient comes from a trailer comparison [15]; ORNL offers a separate stationary analogue [22]. Its escalated 430-bar estimates are 0.832–0.867 of the 1,122 USD/kg reference coefficient and fall within the declared ±30% capital support. This supports the assumed cost scale but does not calibrate that support. Nor do SCCV manufacturing estimates establish matched installed prices for Type I or composite-wrapped vessels. The retained coefficients remain engineering assumptions with qualified literature support. Before procurement, pressure, construction, stored-versus-deliverable capacity, installation, and replication must be reconciled. The 860-bar analogue does not add CG700 to the current economic comparison.

Hydride material feasibility needs separate evidence. A van't Hoff pressure above 20 bar provides an equilibrium screen but does not establish reversible capacity, pressure loss, delivery rate, start-up behavior, or heat-transfer area. The assumed upfront allowance also does not predict degradation with cycling, temperature, or impurities. The hydride case estimates the material and cost burden of an assumed performance target without showing that the target has been met.

The sensitivity and regret results suggest where to collect evidence first. Feasible delivery and restoration must be confirmed before obtaining matched costs for the most influential hardware and refining secondary operating inputs. The model does not simulate outage probabilities, optimize reserve adequacy, or monetize reliability. Extending it to these questions would require an independently supported outage process and a value-of-unserved-hydrogen model. Here, reserve requirements are prescribed design choices. A separate usable-capacity margin experiment estimates the extra gas-vessel burden without assuming a specific unverified pressure margin. Supporting Information S20 records supplier documents and their applicability limits.

12 CONCLUSIONS

Reserve duration alone does not determine the preferred hydrogen-storage technology. The allowed restoration time sets conditioning duty, and available supply and utilities determine whether that duty can be met. In the production-scale benchmark, the 90-day reserve cannot be replenished within the annual cycle under the assumed demand. The cost comparison therefore cannot support a project recommendation. Average-capacity checks also leave minimum stable throughput and chronological operability unresolved.

Within the declared cost models, the gas–liquid crossover moves from about 55 days under the inherited transfer basis to about 9–15 days when stationary sources are substituted. This change in cost structure has a much larger effect than numerical sampling variation. Combined-source worst-case regret favors gas for short reserves and liquid for longer reserves under the stated cost set and operating assumptions. The analysis provides a reproducible way to establish feasible service, reconcile installed cost scope, and assess the consequences of technology selection. Applying these screening results to deployment requires matched supplier estimates, facility records, and independent technical review.

Supporting information

The supplement gives the model coefficients, inventory trajectories, uncertainty definitions, scenario layers, cash-flow and unit checks, and convergence evidence. It separates retained historical results from those of the new model revision. The matching code-and-data archive contains Python evaluators, numerical inputs, draw-level outputs, plotting scripts, tabular results, and run instructions. No public repository DOI has been assigned.

STATEMENTS ON COMPLIANCE WITH ETHICAL STANDARDS

Acknowledgments

We thank the researchers whose published experimental, thermophysical, and technoeconomic studies informed this work.

Disclosure of conflict of interest

If two or more authors have contributed in the manuscript, the conflict of interest statement must be inserted here. When no conflict of interest exists author should write as "The authors declare no conflicts of interest regarding this manuscript".

Statement of ethical approval

If studies involve use of animal/human subject, authors must give appropriate statement of ethical approval. If not applicable then mention 'The present research work does not contain any studies performed on animals/humans subjects by any of the authors'.

Statement of informed consent

If studies involve information about any individual e.g. case studies, survey, interview etc., author must write statement of informed consent as "Informed consent was obtained from all individual participants included in the study."

Author contributions:

Rawail Saeed: Conceptualization, Methodology, Software, Formal analysis, Investigation, Data curation, Validation, Writing – original draft. Syed Zeeshan: Manuscript formatting and preparation.

Declaration of AI-assisted technologies:

During manuscript preparation, the authors used OpenAI ChatGPT for language revision and organization.

Data and code availability

The reference numerical results use the matching model.py, run_analysis.py, and extra_analysis.py workflows. The evidence_analysis.py script computes source-family, eligibility, and combined-box results. The operability_analysis.py script computes revision-5 operating envelopes, scope scenarios, and hourly balances. For traceability, the archive preserves the earlier 10,000-draw input design and provides revised outputs separately. It contains no new laboratory measurements or supplier quotations. Historical arrays remain verification records and are not relabeled as outputs of the revised evaluator. Revision-6 accounting and usable-capacity-margin results are computed by closeout_analysis.py and stored separately.

REFERENCES

[1] International Energy Agency. The Future of Hydrogen. IEA, 2019. https://www.iea.org/reports/the-future-of-hydrogen.

[2] U.S. Department of Energy. Hydrogen Program Records. https://www.hydrogen.energy.gov/library/program-records (accessed 22 October 2026).

[3] D.D. Papadias, R.K. Ahluwalia, Bulk storage of hydrogen, Int. J. Hydrogen Energy 46 (2021) 34527–34541. https://doi.org/10.1016/j.ijhydene.2021.08.028.

[4] X. Wang et al. Technoeconomic Insights into Metal Hydrides for Stationary Hydrogen Storage. Adv. Sci. 12 (2025) 2415736. https://doi.org/10.1002/advs.202415736.

[5] A. Ademollo et al. Comparative techno-economic assessment of stationary hydrogen storage technologies. Int. J. Hydrogen Energy 199 (2026) 152849. https://doi.org/10.1016/j.ijhydene.2025.152849.

[6] U.S. Department of Energy, Energy requirements for hydrogen gas compression and liquefaction as related to vehicle storage needs, Hydrogen Program Record 9013 (2009). https://www.hydrogen.energy.gov/docs/hydrogenprogramlibraries/pdfs/9013_energy_requirements_for_hydrogen_gas_compression.pdf (accessed 22 October 2026).

[7] J.W. Leachman et al. Fundamental Equations of State for Parahydrogen, Normal Hydrogen, and Orthohydrogen. J. Phys. Chem. Ref. Data 38 (2009) 721–748. https://doi.org/10.1063/1.3160306.

[8] I.H. Bell et al. Pure and Pseudo-pure Fluid Thermophysical Property Evaluation and the Open-Source Thermophysical Property Library CoolProp. Ind. Eng. Chem. Res. 53 (2014) 2498–2508. https://doi.org/10.1021/ie4033999.

[9] W. Johnson. Performance Testing of Liquid Hydrogen Tanks. Cold Facts (2024). NASA NTRS 20240000753. https://ntrs.nasa.gov/citations/20240000753.

[10] U.S. Department of Energy, Current status of hydrogen liquefaction costs, Hydrogen Program Record 19001 (2019).

https://www.hydrogen.energy.gov/docs/hydrogenprogramlibraries/pdfs/19001_hydrogen_liquefaction_costs.pdf (accessed 22 October 2026).

[11] Chemical Engineering. CE Plant Cost Index Report. Annual CE Index series 2000–2024. https://www.chemengonline.com/wp-content/plugins/ce-base/views/pci-cost-download.php?From_Year=2000&To_Year=2024&type=year (accessed 24 October 2026).

[12] B. Tarasov, A. Arbuzov, S. Mozhzhukhin, A. Volodin, P. Fursikov, M.W. Davids, J. Adeniran, M. Lototskyy, Metal hydride hydrogen storage (compression) units operating at near-atmospheric pressure of the feed H_2, Inorganics 11 (2023) 290. https://doi.org/10.3390/inorganics11070290.

[13] T. Sato, H. Saitoh, R. Utsumi, J. Ito, Y. Nakahira, K. Obana, S. Takagi, S. Orimo, Hydrogen absorption reactions of hydrogen storage alloy $LaNi_5$ under high pressure, Molecules 28 (2023) 1256. https://doi.org/10.3390/molecules28031256.

[14] G.G. Griñán, T. Gómez-Acebo. Techno-economic analysis of hydrogen storage options using a reproducible software model. International Journal of Hydrogen Energy 258 (2026) 156618. https://doi.org/10.1016/j.ijhydene.2026.156618. Associated equations and MATLAB code: https://doi.org/10.17632/rwzyyfgcpc.3.

[15] G. Petitpas, A.J. Simon, J. Moreno-Blanco. Liquid Hydrogen Infrastructure Analysis. DOE Hydrogen and Fuel Cells Program FY 2017 Annual Progress Report, III.10. https://www.hydrogen.energy.gov/docs/hydrogenprogramlibraries/pdfs/progress17/iii_10_petitpas_2017.pdf.

[16] M.J.W. Jansen. Analysis of variance designs for model output. Computer Physics Communications 117 (1999) 35–43. https://doi.org/10.1016/S0010-4655(98)00154-4.

[17] U.S. Energy Information Administration. Electric Power Annual, Table 2.4, average price by end-use sector. https://www.eia.gov/electricity/annual/table.php?t=epa_02_04.html (accessed 24 October 2026).

[18] V. Semchukova, K. Polemis, Z. Abdin, B. Solanki, S. Cary. Hydrogen Infrastructure Analysis for Port Applications. NREL, October 2024, slide 65. https://docs.nlr.gov/docs/fy25osti/91396.pdf.

[19] C. Houchins, J.H. Prosser, M. Graham, Z. Watts, B.D. James. Hydrogen Storage Cost Analysis. DOE Annual Merit Review, Project ST235, June 2023, slide 9. https://www.hydrogen.energy.gov/docs/hydrogenprogramlibraries/pdfs/review23/st235_houchins_2023_p-pdf.pdf.

[20] C. Houchins, J.H. Prosser, M. Graham, Z. Watts, B.D. James. Hydrogen Storage and Cost Analysis. DOE Annual Merit Review, Project ST235, May 2024, slides 3 and 8. https://www.hydrogen.energy.gov/docs/hydrogenprogramlibraries/pdfs/review24/st235_houchins_2024_o.pdf.

[21] U.S. Department of Energy. May H2IQ Hour Megawatt Scale Tri Gen System Produces Clean Hydrogen Electricity and Water at the Port of Long Beach. Text version, Toyota presentation. https://www.energy.gov/cmei/fuels/may-h2iq-hour-megawatt-scale-tri-gen-system-produces-clean-hydrogen-electricity-and-0 (accessed 24 October 2026).

[22] W. Zhang, F. Ren, Z. Feng, J.-A. Wang. Manufacturing Cost Analysis of Novel Steel/Concrete Composite Vessel for Stationary Storage of High-Pressure Hydrogen. Oak Ridge National Laboratory, DOE Project PD088, September 2012, Tables 1, 8 and 9. https://info.ornl.gov/sites/publications/Files/Pub41882.pdf.

[23] E.M. Chao, M. Chase, K. Jadd. An Economic Analysis of the DTE Energy Hydrogen Technology Park. Master's thesis, University of Michigan, CSS06-10, 2006, Section 3.1. https://hdl.handle.net/2027.42/38882.